Calculation of spectral weighting functions for the solar photobleaching of chromophoric dissolved organic matter in temperate lakes

Christopher L. Osburn[1]

Department of Earth and Environmental Sciences, Lehigh University, 31 Williams Drive, Bethlehem, Pennsylvania 18015

Horacio E. Zagarese

Consejo Nacional de Investigaciones Cientificas y Tecnicas, Bariloche, Argentina

Donald P. Morris and Bruce R. Hargreaves

Department of Earth and Environmental Sciences, Lehigh University, 31 Williams Drive, Bethlehem, Pennsylvania 18015

Walter E. Cravero

Departamento de Fisica, Universidad Nacional del Sur, Alem 1253 Bahia Blanca, Argentina

Abstract

The effect of solar radiation on the dissolved absorption coefficient ($a_{CDOM}[\lambda]$), which reflects the concentration of chromophoric dissolved organic matter (CDOM), was investigated in several lakes near Bariloche, Argentina and in northeastern Pennsylvania, USA. Samples of 0.2 μm filtered lake water were exposed in quartz tubes to different portions of the solar spectrum using optical cutoff filters to remove parts of the ultraviolet (UV) region of the solar spectrum. Changes in the spectral absorption in these samples and the absorbed incident energy were used to calculate spectral weighting functions (SWFs) for the photobleaching (PB) of CDOM. PB was measured as the loss of $a_{CDOM}(\lambda)$ (the $a_{CDOM}[\lambda]$ was averaged from 280 to 500 nm) per unit absorbed energy. CDOM from humic and clear lakes, as well as from a *Sphagnum* bog and an algal culture, was used in the experiments covering a wide range of carbon sources. We used an iterative, nonlinear optimization method to fit the measured results to a simple exponential function in order to generate each SWF. Comparing individual SWFs calculated for various CDOM sources, we computed a summary SWF from the experiments using epilimnial CDOM from our study lakes. Our summary SWF was able to explain 80–90% of the observed variance in our exposure experiments, and we were able to predict PB results obtained for other Argentine lakes (mean error 14.5%). Finally, we calculated that the effect of UV-B radiation on PB was small (<20% of total decrease in the absorption coefficient) compared to UV-A and blue light radiation. This suggested that increased UV-B radiation due to stratospheric ozone depletion would not greatly increase the photobleaching of whole water column CDOM in Patagonian lakes (<10%).

The susceptibility of lake ecosystems to solar ultraviolet radiation (UVR) has recently received much study. Many workers have demonstrated the ability of UVR to affect the biota of lakes, as well as their physical environment (Karentz et al. 1994; Williamson and Zagarese 1994; Morris and Hargreaves 1997). One important consequence of this research is the realization of seasonal variability in the transmission of UVR through the water column of lakes (Morris and Hargreaves 1997). This variation is most likely due to photobleaching, a process that has been shown to increase the transmission of UVR through the water column by degrading the ability of certain materials (e.g., chromophoric dissolved organic matter, CDOM) to absorb UV radiation. The resulting effect could expose a larger proportion of a lake's water column to higher levels of UVR, particularly in the UV-B region (280 to 320 nm), which is the most biologically damaging portion of the solar spectrum (cf. Karentz et al. 1994). Of particular concern is the possibility that increased UVR reaching the Earth's surface from stratospheric ozone depletion may result in a higher UVR environment in lakes. Hader and Worrest (1991) and Hader et al. (1998) discussed the potential impact of UVR to aquatic food webs, suggesting that multiple trophic levels may be affected. They note that even a modest increase in UV-B radiation can impact the development of commercially important organisms such as fish and shellfish, which have larval stages residing near the surface of aquatic ecosystems. Thus, it is important to understand how higher fluxes of UVR at the Earth's surface might affect the optical properties of lakes.

The effects of UV-B radiation are the most pronounced and raise the most concern in studies of biological systems. However, evidence from experimental studies of photobleaching of CDOM in lake water and from field measure-

ments of changes in lake optical properties suggests that wavelengths other than the UV-B region may be more important to the photobleaching of CDOM (Morris and Hargreaves 1997; Graneli et al. 1998; Vähätalo et al. 2000). A prerequisite to our understanding of photobleaching is a knowledge of the relative degree to which portions of solar spectrum are responsible for the loss of UV absorbance and the subsequent increase in water column transparency. This is especially true for models that predict increases in water column transparency due to stratospheric ozone depletion, which results only in increases in UV-B fluxes. In their analysis of photobleaching of lake water in three lakes in northeastern Pennsylvania, USA, Morris and Hargreaves (1997) determined rate constants for loss of dissolved absorbance under three different light treatments. They reported loss of dissolved absorbance in treatments shielded from most of the UVR (wavelengths <377 nm) and suggested that wavelengths greater than 377 nm contributed up to 7% of the loss of dissolved UV absorbance. Similar results were found by Reche et al. (1999). Thus, the photobleaching effectiveness of wavelengths in both the UV and the lower PAR (photosynthetically active radiation, 400–700 nm) regions requires analysis.

In this study, we analyzed the spectral dependency of CDOM photobleaching (as a decrease in the dissolved UV absorption coefficient) by natural sunlight through the development of spectral weighting functions (SWF). A SWF is a mathematical expression that weights the energy per photon (in J m^{-2}) of UVR to cause some effect (in this case, photobleaching of DOM) based on the relative effectiveness of different wavelengths.

The SWF is similar to biological weighting functions (BWFs) that have been calculated for numerous ecosystem processes. Weighting functions exist for biological processes such as inhibition of photosynthesis (Cullen et al. 1992; Boucher and Prezelin 1996; Cullen and Neale 1997), DNA damage (Setlow 1974; Karentz et al. 1994), and for chemical processes such as the generation of low molecular weight (LMW) carbonyl compounds (Kieber et al. 1990) and hydrogen peroxide (Moran and Zepp 1997). Rundel (1983) and Cullen and Neale (1997) provide reviews of the methodology involved in calculating a weighting function.

The goal of this study was to calculate and validate SWFs for photobleaching, which were determined as a loss of dissolved absorbance averaged over the wavelength band of 280–500 nm. We also wanted to determine whether a summary SWF could be used to predict photobleaching of CDOM from different lake ecosystems. We report SWFs for, and compare the photoreactivity of, CDOM from several different lakes located in the Nahuel Huapi National Park (Rio Negro, Argentina) and on the Pocono Plateau of northeastern Pennsylvania, USA. Thus, we had a contrast between clear and humic temperate lakes from the northern and southern hemispheres.

Methods

Study Site—Water samples from two lakes in Argentina and two lakes in Pennsylvania were used to construct the

Table 1.   Description of symbols and abbreviations.

A	Spectrophotometer absorbance (unitless)
$a_{CDOM}(\lambda)$	Dissolved absorption coefficient of CDOM at wavelength (m^{-1})
$a_{CDOM}(\lambda)_{avg}$	Geometric average of initial and final CDOM absorption coefficients (m^{-1})
$a_{CDOM}(\lambda)_{init}$	Initial CDOM absorption coefficient (m^{-1})
$a_{CDOM}(\lambda)_{treat}$	Final CDOM absorption coefficient after exposure (m^{-1})
BWF	Biological weighting function
E	Energy (J m^{-2})
$E_d(\lambda)$	Downward incident energy at λ (J m^{-2})
$E_a(\lambda)$	Absorbed energy at λ (J m^{-2})
$E_{photon}(\lambda)$	Energy per photon at λ (J m^{-2})
$K_d(\lambda)$	Diffuse attenuation coefficient at λ (m^{-1})
λ_{eff}	Wavelength of most effective photobleaching (nm)
PB(λ)	Photobleaching measured as a loss of dissolved absorbance at λ (m^{-1})
PB$_{meas}$	Measured photobleaching summed over the wavelength range of 280 to 500 nm (m^{-1})
PB$_{pred}$	Predicted photobleaching summed over the wavelength range of 280 to 500 nm (m^{-1})
$W(\lambda)$	Spectral weight of photobleaching effectiveness at λ (m J^{-1})

SWFs. A summary of limnological and optical characteristics of the study lakes is presented in Table 2 and shows the variation in DOM concentration (measured as dissolved organic carbon, DOC) and UVR absorbance. Lake Trebol is a small, humic lake located near Bariloche, Argentina (41°05′S, 71°30′W; elev. 430 m) in the mountainous Patagonian region of South America. This lake is dimictic and experiences thermal stratification during the Austral summer. The lake is surrounded by a small, forested watershed and has abundant macrophytes growing in the littoral zone that provide a source of DOM to this lake (DOC concentration is 1.7 mg L^{-1}). Similarly, Lake Lacawac is a small, dimictic lake in Pennsylvania (41°22.95′N, 75°17.58′W; elev. 122 m; DOC concentration is 4.80 mg L^{-1}) surrounded by a *Sphagnum* bog. We assumed that the CDOM in both Lacawac and Trebol is derived primarily from plant materials and thus similar to the bog CDOM. In contrast, Lake Moreno East is a large, clear, and warm monomictic lake with less DOC (0.65 mg L^{-1}). Lake Giles is a clear dimictic lake located about 20 km from Lacawac, with a DOC concentration similar to Lake Trebol (1.09 mg L^{-1}). The CDOM in Moreno East and Giles is assumed to be derived mainly from autochthonous primary productivity rather than from watershed sources.

Optically, the lakes exhibit a wide contrast in UV attenuation. Lake Lacawac has the largest UV absorption coefficient, followed by Lake Trebol (Table 2). Lake Giles and Lake Moreno East are more transparent to UVR. These variations demonstrate the range of lake types used in this study and underscore the heterogeneity in CDOM from humic and clear lakes.

Argentina experimental design—In our photobleaching experiments, we used a series of nine Schott optical low-cutoff filters that transmit increasingly complete solar spec-

Table 2. Summary of optical and chemical parameters for the study lakes from North and South America. Note that Trebol and Escondido have much higher DOC concentrations than Moreno East or Nahuel Huapi, and thus higher UV attenuation. Chl *a* as mg m^{-3}; DOC as g m^{-3}; $a_{CDOM}(\lambda)$ and K_d as m^{-1}. Data are from Morris et al. (1995).

Lake (country)	Chl *a*	DOC	$a_{CDOM}(320)$	$K_d(320)$	$a_{CDOM}(380)$	$K_d(380)$
Trebol (ARG)	0.90	1.70	0.88	3.29	0.20	1.54
Escondido (ARG)	0.20	2.66	2.81	7.68	0.83	3.03
Moreno East (ARG)	0.25	0.65	0.22	0.52	0.06	0.23
Nahuel Huapi (ARG)	0.10	0.24	0.20	0.49	0.05	0.23
Giles (USA)	0.64	1.16	0.10	0.32	0.03	0.16
Lacawac (USA)	2.72	4.67	2.50	7.78	0.63	3.22

tra. We assumed that the transmission of the cutoff filters was the same in the lab and in the field. Spectral transmission of each filter was measured on a Shimadzu UV-visible spectrophotometer and we determined the following 50% transmission values for the nine filters: 288, 303, 317, 332, 339, 357, 375, 389, and 395 nm. In total, we used nine optical treatments and a dark control; each comprised of five replicates. Water was collected from each lake (2 m in Trebol; 10 m in Moreno East) and filtered sequentially through prerinsed Whatman GF/F glass fiber filters and polysulfone Millipore Sterivex (0.22 μm) filters. We added 0.025% (vol/vol) sodium azide (NaN$_3$) as a bacterial inhibitor. NaN$_3$ absorbs light in the UV region only below 280 nm and we ran independent light and dark exposures of filtered water from Lake Lacawac in quartz tubes with and without addition of NaN$_3$. We observed no difference in loss of absorbance between the samples with and without addition of NaN$_3$, nor did we find any difference between the dark samples. Thus, we concluded that NaN$_3$ added to our samples did not interfere with our absorbance measurements. Samples were placed in flanged quartz test tubes (15 cm length $\times$ 2 cm diameter, optical pathlength $= 0.0177$ m, *see below*) and sealed with silicone stoppers wrapped in acid-washed Teflon tape. The tape excluded potential contamination of the sample from compounds shown to leach from silicone (Lindell and Rai 1994). The quartz tubes used in the experimental exposures were 99% pure, transmitting well below 280 nm. The tubes were initially combusted (450°C, 4 h) and then acid-washed and autoclaved between successive experiments.

Exposure of the Argentine lake CDOM samples to natural sunlight took place at the Laboratorio de Fotobiologia approximately 15 km south of Bariloche, Argentina from December 1998 to February 1999. Samples of CDOM were collected at 2 m in Trebol and at 10 m in Moreno East. The five replicates for each treatment were placed in black plastic boxes that were painted flat black on the inside to minimize reflectance, covered with the appropriate filter, and floated horizontally at the surface of a 200-liter tank filled with water. The water was changed daily and served as a constant temperature bath. We ran four exposures of lake water, three for Trebol (referred to as Trebol 1, 2, and 3), and one for Moreno East, each varying from 5 to 8 d. After the exposure period, samples were transferred to ashed 50 ml borosilicate archive vials and stored in the dark at 4°C until returned to Lehigh University for analysis.

Pennsylvania experimental design—Exposure of the Pennsylvania lake CDOM took place in the surface of Lake Giles during 1998 and 1999 using a similar design. Samples for photobleaching experiments were collected from 1 (epilimnion), 8 (metalimnion), and 10 m (hypolimnion) depths in humic Lake Lacawac on 22 June 1999, 23 July 1998, and 8 July 1999, respectively. Samples were also collected in Lake Giles from 3 m (epilimnion) on 18 July 1999 and 17 m (hypolimnion) on 2 July 1998 and 26 July 1999. We used both surface water samples and deep water samples to determine whether previous photobleaching of CDOM would produce discernible differences in SWFs, because Morris and Hargreaves (1997) have shown that extensive photobleaching occurs in the epilimnia of these lakes. In these experiments, the quartz test tubes were placed in the black boxes, which were affixed to a rack floating at the surface of Lake Giles, and exposed to sunlight. The five replicates were placed in each box, filled with Lake Giles surface water, and covered with an optical cutoff filter, or black plastic (dark control). The frame was floated horizontally in the lake with pontoons situated far enough from the boxes so as not to shade the tubes and to provide stabilization. The rack floated at a depth of approximately 2 cm below the surface of Lake Giles and the depth from the filters to the tubes was an additional 0.5 cm.

Attenuation coefficients of Lake Giles water were estimated from irradiance depth profiles performed with a Biospherical PUV-501 radiometer (depth resolution <1 cm). The diffuse attenuation coefficient (K_d, Kirk 1994) at four wavelengths (305, 320, 340, and 380 nm) was calculated as the slope of Ln (irradiance, μW cm^{-2} nm^{-1}) versus depth (m) in the mixed layer of the water column after correcting data for dark offset values. Typically, the K_d of Lake Giles water is low compared to other lakes (Morris et al. 1995). During 1999, $K_{d,305}$ in Lake Giles decreased from early June ($K_{d,305} = 0.960$) to late July ($K_{d,305} = 0.645$). At a depth of 2 cm the surface irradiance was reduced by 1–2% at 305 nm, thus we did not correct for that attenuation in our experiments. We did not measure photobleaching of CDOM in the overlying water during the exposure period, but K_d was found to decrease by 0.04 m^{-1} per day during June and July 1999; this would cause an increase of less than 0.2% per day for incident irradiance.

In May of 1998, we collected groundwater from a depth of approximately 1.5 m in the *Sphagnum* bog that surrounds nearly one-third of Lake Lacawac to use as an allochthonous

CDOM end member. We also collected algal and microbially generated CDOM from an algal culture grown in low DOM spring water. The algal culture began as an inoculum from Lake Lacawac but shifted to an assemblage dominated by a coccoid chlorophyte. This CDOM sample served as an autochthonous end member. The Pennsylvania lake CDOM samples were exposed in a similar manner described above for the Argentine lakes, but without the addition of azide due to the availability of sterile laboratory equipment (e.g., a laminar flow hood), which reduced bacterial contamination during our exposures.

Irradiance measurements—Solar radiation for experiments conducted in Argentina was measured with a Biospherical Instruments Model 511-C GUV radiometer situated on the roof of the Laboratorio. In Pennsylvania, the solar radiation was measured with a Biospherical Instruments Model GUV-521 radiometer installed at a weather station near Lake Lacawac. Spectral irradiance at five wavelength channels (305, 320, 340, and 380 nm and PAR) was recorded at 1-min intervals in Argentina and for 15-min integrated intervals in Pennsylvania.

A spreadsheet model was used to generate a cumulative solar spectrum (280 to 500 nm) for each exposure period. A series of model reference spectra from 280 to 500 nm (Madronich model described in Kirk et al. 1994) were integrated over a day for low and high ozone values. The reference spectra were generated at 15–30-min intervals for average conditions at Bariloche, ARG on 17 December 1997. For each experiment the resulting low and high ozone pair of daily model spectra were used to fit an experiment spectrum to the daily integrated GUV measurements at the four recorded channels (305, 320, 340, and 380 nm—Morris and Hargreaves 1997). Fitting a daily experiment spectrum involved interpolation between the low and high ozone daily reference spectra to optimize the match with integrated GUV measurements (first for UV-A to account for cloud density and then for UV-B to account for ozone). This approach has been shown to generate spectra that compare favorably to solar spectra measured with double monochrometer scanning radiometers (Kirk et al. 1994). The daily irradiance spectra are summed over the exposure period (5 to 8 d) to calculate the total cumulative irradiance (μW cm^{-2} nm^{-1}) for each experimental exposure. The cumulative irradiance was then converted to incident energy (E_d; J m^{-2}; *see Table 1 for notation used*) to provide a cumulative exposure for each treatment.

The effective pathlength of solar irradiation through the quartz test tube was calculated as 0.0177 m, the square root of the quartz tube's measured area. The pathlength through each tube was computed as the average distance of any number of straight lines bisecting a 2 cm length square at any angle from vertical, which we assume represents the average pathlength of a photon. This distance is 2 cm, which is also the square root of the square's area. Applying this reasoning to a circle (representing the cross section of the 2 cm quartz tube), the square root of the area of a circle with a diameter of 2 cm should be slightly less than 2 cm, or $(\pi \times [1 \text{ cm}]^2)^{1/2}$ = 1.77 cm = 0.0177 m. We considered the tubes to be optically thin at this pathlength (e.g., the energy at 320 nm

absorbed during each experiment of Trebol and E. Moreno water ranged from 1–4% of initial E_d).

Measurements of CDOM optical density ($A[\lambda]$) were made on a Shimadzu UV160 spectrophotometer and converted to the dissolved absorption coefficient ($a_{CDOM}[\lambda]$) calculated according to Kirk (1994):

$$a_{CDOM}(\lambda) = 2.303A(\lambda)/l, \qquad (1)$$

where λ is wavelength, in nanometers, and l is the pathlength, in meters. The $a_{CDOM}(\lambda)$ of CDOM from each sample was corrected for $a_{CDOM}(\lambda)$ absorbance of pure water by subtraction of $a_{CDOM}(\lambda)$ measured for a low-carbon DI water blank. When sodium azide was used as a microbial inhibitor (i.e., the Argentina exposure experiments), it was added to this blank in the same concentration used in the sample treatments.

Overview of weighting function calculations—The SWFs for each experiment were determined by an iterative nonlinear regression fit of a simple exponential function that weights wavelengths from the range of 280 to 500 nm for their effectiveness to photobleach CDOM. The weights were determined by linear regression of the integrated photobleaching in each spectral treatment versus the total cumulative absorbed energy in each treatment for each experimental exposure. This method requires the assumption of a particular shape to the weighting function, which we achieved with initial estimates for the slope and for the weight (the photobleaching effect per nm, $W[\lambda]$) at a reference wavelength, in this case 300 nm. The value $W(\lambda)$ is defined as the loss of absorbance per unit absorbed energy per nm, resulting in units of m J^{-1}. We chose 300 nm as the reference wavelength based on Rundel (1983). During each iteration, the weights were adjusted to optimize the fit of a nonlinear regression of the observed photobleaching data to the energy absorbed in each treatment. We assumed a simple exponential form for the weighting function based on the exponential relationship of the absorption coefficient versus wavelength for natural waters and based on the approximately exponential increase in photon energy with decreasing wavelength. Further, recent studies of CDOM photobleaching and DOC photomineralization in natural waters have also reported quantum yields (QY), which decrease exponentially with wavelength (cf. Kieber et al. 1990, Valentine and Zepp 1993, Vähätalo et al. 2000, and Whitehead et al. 2000—apparent QY).

We used the spectral slope (S) of each lake water sample as a seed value for the slope of the SWF (S_w). The spectral slope for each water sample was calculated as the slope of the natural log of $a_{CDOM}(\lambda)$ versus wavelength, over the range of 280 to 500 nm. The seed value for the weight at 300 nm ($W300$) was estimated from a regression of the differential photobleaching calculated for adjacent filter treatments versus the differential absorbed energy in adjacent treatments. We note here that modeling efforts for BWFs (most notably for DNA; Setlow 1974) also employ simple exponential functions.

Measured photobleaching (PB$_{meas}$, m^{-1}) of CDOM exposed to natural sunlight was computed from dissolved ab-

sorption coefficients as the loss of absorbance averaged over the range of 280 to 500 nm

$$PB_{meas} = \frac{\sum\limits_{\lambda=280}^{500} a_{CDOM}(\lambda)_{init} - a_{CDOM}(\lambda)_{treat}}{220}, \quad (2)$$

where $a_{CDOM}(\lambda)_{init}$ is the initial dissolved absorption coefficient at λ (corrected for dark controls), and $a_{CDOM}(\lambda)_{treat}$ is the final dissolved absorption coefficient at λ measured in each filter treatment. Our use of averaged absorbance loss (or fading) of the entire UV and blue light absorbance of CDOM is similar to other studies of photobleaching (Whitehead et al. 2000) and lake color (Hongve and Åkesson 1996; Molot and Dillon 1997). In doing so, we note that a limitation of this approach is the difficulty in comparison with action spectra constructed from single wavelength responses using monochromatic radiation. Such spectra are usually derived from analyses of single compounds (e.g., DNA, Setlow 1974). Nonetheless, we feel that spectrally integrated absorbance loss offers a useful representation of changes to the dissolved absorbance spectrum under polychromatic radiation. Our approach avoids introducing a bias from the response, observed in studies of monochromatic action spectra as both a "local" loss of absorbance at the irradiation wavelength, and a "global" loss at other wavelengths (cf. Allard et al. 1994, their fig. 2, and discussions by Kouassi and Zika 1992 and Whitehead et al. 2000).

The absorbed energy in each treatment ($E_a[\lambda]$, J m^{-2}) was calculated by computing the difference between energy entering and passing through the quartz tubes, following the recommendations of Miller (1998). We calculated $E_a(\lambda)$ based on the following equation:

$$E_a(\lambda) = E_d(\lambda) - E_d(\lambda) \cdot \exp(-a_{CDOM}[\lambda]_{avg} \cdot 0.0177), \quad (3)$$

where $E_d(\lambda)$ is the spectrum of incident energy (J m^{-2}) per nm increment of wavelength in each filter treatment, $a_{CDOM}(\lambda)_{avg}$ is the geometric mean of the initial and final dissolved absorption coefficients at each wavelength, and 0.0177 is the optical pathlength of the quartz tube, in meters. Over short pathlengths and in weakly absorbing solutions, the exponential relationship approximates a linear relationship and Eq. 4 may reduce to

$$E_a(\lambda) = E_d(\lambda) \cdot (a_{CDOM}[\lambda]_{avg}) \cdot 0.0177. \quad (4)$$

The geometric mean of initial and final absorption coefficients approximates the change in CDOM absorbance (assumed to decrease exponentially) with sunlight exposure (Zepp 1988; Miller and Zepp 1995). The absorbed energy is necessary to calculate the weight, $W(\lambda)$, which expresses the effect per unit energy absorbed resulting in decreased absorbance. In this case, the effect is PB, the loss of absorbance averaged from 280 to 500 nm.

We used an iterative nonlinear regression model developed by Patrick Neale for the SAS system (SAS Institute) to compute the best-fit parameters to the following equation:

$$W(\lambda) = W300 \cdot \exp(-S_w[\lambda - 300]), \quad (5)$$

where $W(\lambda)$ is the weight (in m J^{-1}) at λ, $W300$ is the weight at 300 nm, and S_w is the slope of the exponential. The iterative regression changes $W300$ and S_w from seed values until the best fit of observed data is achieved. This equation is similar to others used to generate absorption coefficients at wavelength from measured optical data using the spectral slope (Bricaud et al. 1981; Kirk 1994; Vodacek et al. 1997). Using the resulting SWF, we calculated predicted photobleaching (PB$_{pred}$, m^{-1}) by multiplying the absorbed energy ($E_a[\lambda]$) at each wavelength by its modeled $W(\lambda)$, which converts the absorbed energy at that wavelength to the photobleaching effect at that wavelength:

$$PB_{pred} = \sum\limits_{\lambda=280}^{500} Ea(\lambda) \cdot W(\lambda). \quad (6)$$

The summation of effects over the wavelength range of 280 to 500 nm equals our prediction of photobleaching, PB$_{pred}$.

We tested the predictive ability of each SWF in two stages. First, we used each of three calculated SWFs for Lake Trebol CDOM to predict photobleaching in a fourth exposure of Lake Trebol CDOM that was not used to calculate a SWF. Second, we used a summary SWF (the average of the SWFs calculated for surface water samples from all lakes studied) to predict photobleaching of CDOM from a variety of lakes.

Results and discussion

Photobleaching of CDOM from various sources—The cutoff filter experiments using CDOM from various sources show progressive photobleaching (PB$_{meas}$) in treatments that included more UVR. Figure 1 shows the results of the cutoff filter experiments and the variability in response among lakes. There was little difference in PB$_{meas}$ among treatments within the UV-B region ($\sim$0.2 m^{-1} for Lacawac, $<$0.05 m^{-1} for all others), which is not surprising given the small difference in energy corresponding to these successive filter treatments. Moreover, the results suggest a linear, or a very slightly exponential, increase in PB$_{meas}$ with increasing absorbed energy.

When PB$_{meas}$ for the Trebol exposure was plotted against the 50% transmission value for each filter, it is easy to see that the greatest rate of change in PB$_{meas}$ occurred between filters that included successively more UV-A radiation (Fig. 2). However, the results do indicate that UV-B radiation is effective in photobleaching lake water CDOM since the most photobleaching was observed in filter treatments which included nearly all environmentally relevant UV wavelengths (i.e., full sun).

We note that a decreased cutoff wavelength does not necessarily lead to a proportional increase in PB$_{meas}$ (Fig. 2). Little change ($\sim$0.05 m^{-1}) occurred between the 288 nm and 303 nm UV-B filters, suggesting that inclusion of low wavelength, high-energy UV-B (between 280 and 300 nm) was of a small enough quantity as to not have a measurable effect. In fact, the maximum effect was often observed in the 303 nm cutoff filter, probably due to very small difference in transmitted energy between these adjacent filters. Thus,
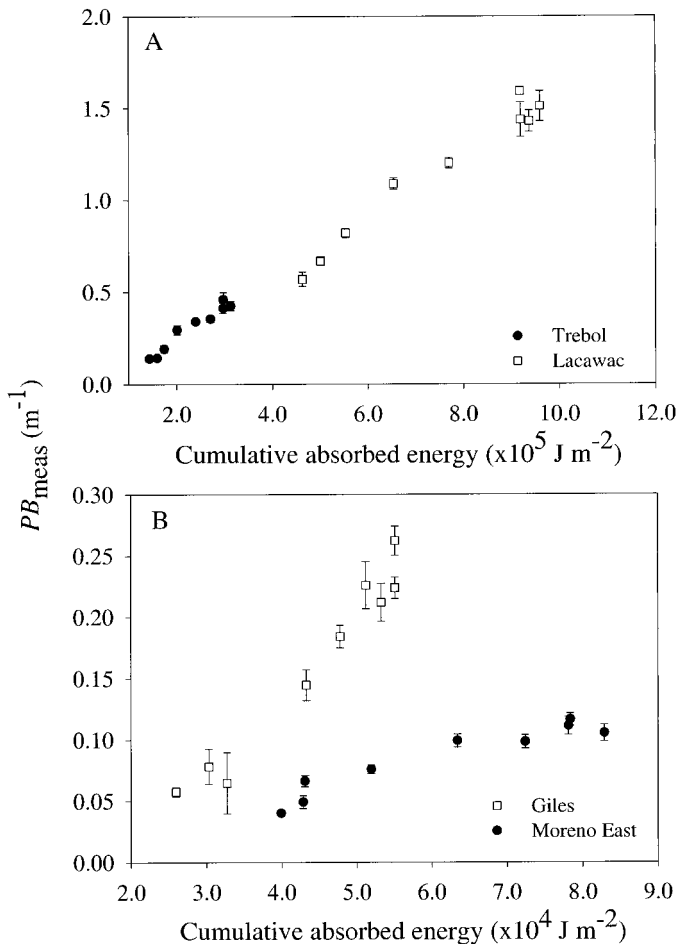
Fig. 1. Photobleaching results from approximately 7-d surface exposures of CDOM from (A) humic Lakes Trebol and Lacawac and (B) clear Lakes Moreno East and Giles to solar UVR. In general, increased amounts of energy caused more integrated photobleaching (from 280 to 500 nm [PB$_{meas}$]). Note variation in cumulative absorbed energy between humic and clear lakes. Error bars are 95% confidence intervals that represent intertube variability between five replicates.

we did not include the 288 nm cutoff filter results in the calculation of SWF from exposure of CDOM sources.

Interaction of multiple wavelengths in CDOM photobleaching—Figure 3 demonstrates the phenomenon of multiple wavelength interactions by showing the loss of absorbance at 320 nm (a_{CDOM}[320]) in each filter treatment plotted against the incident energy at 320 nm (E_d[320]) in each treatment. The treatments with less than 1×10^3 J m^{-2} transmit <1% at 320 nm but clearly show loss of absorbance of roughly 50% of that lost in treatments transmitting 30–100% at 320 nm. Our results indicate that the loss of absorbance at any one part of the spectrum may be due to energy absorbed at other parts of the spectrum. Whitehead et al. (2000) also observed CDOM photobleaching at wavelengths below which there were no incident energy measured. Although the longer wavelength UV-A cutoff treatments transmitted very little energy at 320 nm, we observed a decrease in
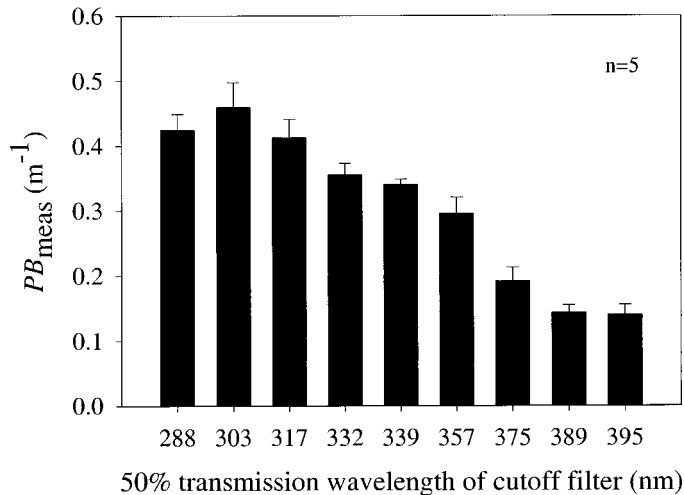

Fig. 2. Photobleaching in the Trebol 2 experiment versus the 50% transmission wavelength measured for each cutoff filter treatment. Error bars represent the 95% confidence intervals.

a_{CDOM}(320). In fact, nearly 50% of the absorbance loss observed in the UV-B filter treatments was measured in the UV-A filter treatments (Fig. 3). Thus, absorbance loss at any one wavelength is apparently due to photons from multiple wavelengths. Although photobleaching may be wavelength specific in terms of absorption of photons (a quantum effect), our data suggest that multiple wavelengths have the ability to photobleach CDOM absorbance measured at any single wavelength. This complicates the application of photobleaching action spectra derived from monochromatic radiation to CDOM photobleaching in the natural environment,
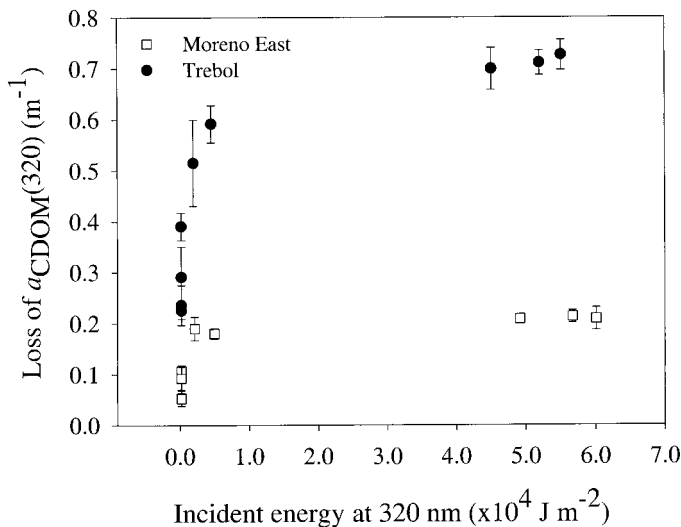

Fig. 3. Loss of CDOM absorbance at 320 nm (a_{CDOM}[320]) versus incident energy at 320 nm (E_d[320]) transmitted through the filters for all experimental treatments in Lake Trebol and Lake Moreno East. Nearly half the total loss of a_{CDOM}(320) measured for the UV-B filter treatments was measured for the UV-A filter treatments (357, 375, 389, and 395 nm), which received roughly 1% of the E_d(320) transmitted through the UV-B filters.
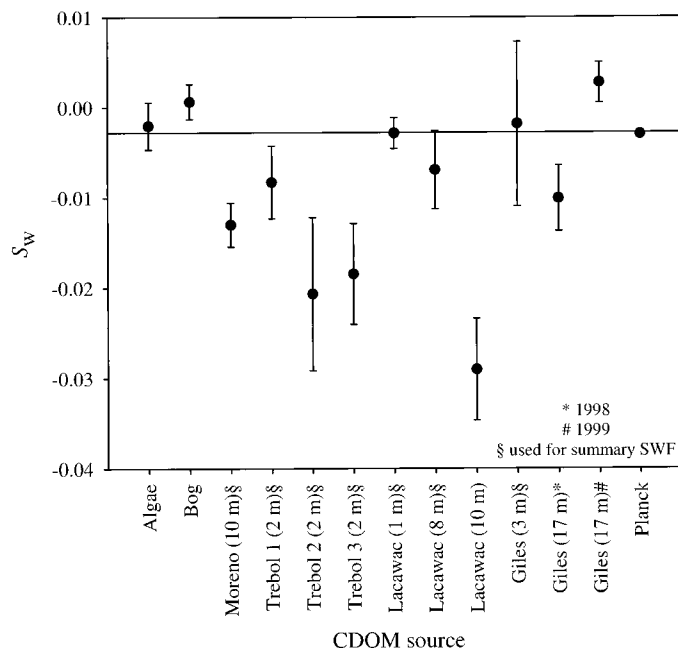
Fig. 4. Variation in SWF slopes (S_w) using CDOM from several lakes, a bog, and an algal culture. The slope calculated for Planck's relationship is also plotted for comparison and marked with a horizontal line. § denotes SWFs used to calculate the summary SWF from epilimnion CDOM samples. Error bars represent 95% confidence intervals ($n = 3$–5).

where aquatic ecosystems are exposed to polychromatic natural sunlight.

Variation in calculated SWFs—Figure 4 shows the slope of each SWF (S_w) we calculated along with its 95% confidence interval. Most of the SWFs had slopes with overlapping 95% confidence intervals. The Argentina lakes exhibited some variation in S_w (-0.008 to -0.021) but did not vary significantly from one another, or from the Giles hypolimnion sample from 1998. The S_w for the Lacawac hypolimnion was the most negative of all SWFs calculated (-0.029). Two SWFs (bog and Giles hypolimnion from

Table 3. Weights at 300 nm (W300) for calculated SWFs, along with regression coefficients and most effective wavelength for photobleaching (λ_{eff}).

| CDOM Source	W300	r^2	λ_{eff}
Algae culture	5.10×10^{-6}	0.82	330
Lacawac bog	4.94×10^{-6}	0.92	330
Lacawac epilimnion	2.10×10^{-6}	0.94	330
Lacawac metalimnion	3.24×10^{-6}	0.86	330
Lacawac hypolimnion	3.42×10^{-5}	0.89	330
Giles epilimnion	3.98×10^{-6}	0.52	330
Giles hypolimnion (98)	1.01×10^{-6}	0.89	330
Giles hypolimnion (99)	2.32×10^{-6}	0.86	330
E. Moreno epilimnion	4.08×10^{-6}	0.93	335
Trebol epilimnion 1	2.27×10^{-6}	0.86	330
Trebol epilimnion 2	7.06×10^{-6}	0.85	329
Trebol epilimnion 3	7.12×10^{-6}	0.81	330
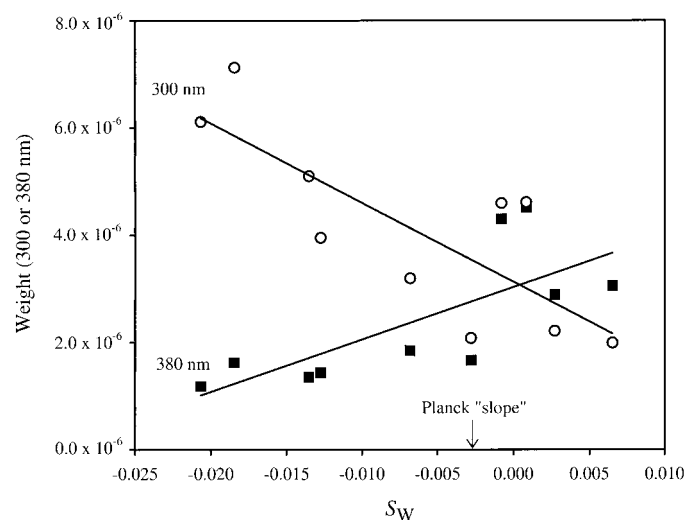
Fig. 5. Relationship between the modeled weights (UV-B and UV-A photoreactivity in m J^{-1}) and the slope for each SWF. The Planck "slope" is indicated for comparison.

1999) had slopes that were slightly positive (0.0006 and 0.0027, respectively) but not significantly different from zero. Moreover, several slopes were not significantly different from the "slope" of the Planck equation, which we approximated by fitting photon energy from Planck's Law to an exponential function of wavelength ($r^2 = 0.994$):

$$\ln E_{\text{photon}}(\lambda) = ae^{-S(\lambda)}, \tag{7}$$

where $E_{\text{photon}}(\lambda)$ is the energy per photon in J m^{-2}, a is a constant, and S is a slope (-0.0026) that is similar to the spectral slope of the exponential absorbance spectrum of CDOM from natural waters.

We compared S_w to the Planck "slope" because quanta of UV-B wavelengths have more energy available for photobleaching than quanta of UV-A or PAR wavelengths. In addition, a given amount of absorbed energy from UV-B photons may be more effective in photobleaching than the same total amount of absorbed energy from a larger number of photons at longer wavelengths. Thus, if the photobleaching effect of natural sunlight is driven primarily by the energy per quantum, we may expect that the SWF will have a slope not significantly different from the Planck slope. Studies are planned to investigate the reaction mechanisms in more detail.

Table 3 presents the W300 data for each individual SWF, along with the regression coefficients for the fit of the PB$_{pred}$ with the PB$_{meas}$ and the most effective wavelength for photobleaching (λ_{eff}). The W300 and the slope were the adjustable terms in the nonlinear regression routine and the r^2 provides an estimate of how well our SWF fit the measured results for each individual SWF calculation. We observed an order of magnitude difference in the range between the W300s calculated for all CDOM sources (2.10×10^{-6} to 3.10×10^{-5}) with an average W300 of 6.97×10^{-6}. The highest W300 was calculated for the Lacawac hypolimnion SWF, whereas the lowest W300 was calculated for the Giles hypolimnion SWF.

Figure 5 shows two trends that may begin to explain the

variation in *W*300. In general, UV-B photoreactivity (*W*300) tends to increase with steepness of S_w ($r^2 = 0.54$), whereas UV-A photoreactivity (W380) tends to decrease with steepness of S_w ($r^2 = 0.62$). This trend implies that the SWFs differ by rotation around a midpoint somewhere in the UV range.

The other trend is that, for most samples, S_w is actually different from that estimated from the Planck slope (-0.0026), which may result from several factors. One is the potential for particular chromophores to differ in their UV reactivity. In this case, destruction of some chromophores requiring less energy (and statistically more likely to be broken by the greater abundance of UV-A photons) could shift the CDOM absorbance to a higher UV-B photoreactivity. Alternatively, it may be that the assemblage of chromophores in "fresher" (i.e., less photobleached) CDOM have a stronger UV-B reactivity. In both instances, the resulting SWF may have a slope steeper than the Planck slope. A third possibility is that the relative abundance of carbon bonds absorbing in either the UV-B or UV-A region changes with photobleaching. Though our data are not conclusive on these points, we note that further experiments comparing the changes in SWF slopes calculated from natural waters to the Planck slope might elucidate the chemical reactions that underlie CDOM photobleaching.

Regression coefficients also varied widely among SWFs calculated. The Lacawac epilimnion SWF had the highest proportion of explained variance ($r^2 = 0.94$), while the Giles epilimnion SWF had the least ($r^2 = 0.52$). The average r^2 for all CDOM sources was 0.85.

We determined λ_{eff} by examining the product of the cumulative energy spectrum and the SWF spectrum. The wavelength at the peak of this spectrum was determined to be λ_{eff} (Table 3). From this spectrum, we found that the largest $PB_{pred}(\lambda)$ occurred in a narrow waveband in the spectrum centered on 330 nm and ranging from 329 to 335 nm.

Determination and functionality of the summary SWF—We wanted to generate a summary SWF that could be used to predict CDOM photobleaching in independent experiments for a variety of lakes. Since most of the predictions were to be made for CDOM from the epilimnia of lakes, we averaged the individual SWFs obtained from epilimnia CDOM samples (i.e., samples having a similar photobleaching history). The average ($\pm$SD) S_w for these SWFs was -0.0103 (± 0.006) and the average *W*300 was 4.34×10^{-6} ($\pm 1.79 \times 10^{-6}$). A chi-square test between each of the S_w and *W*300 values with the calculated mean indicated no significant difference ($\chi^2 < 0.05$). Figure 6 shows the summary SWF, along with the 95% confidence intervals. There is roughly a twofold difference in $W(\lambda)$ between the UV-B and UV-A and blue light wavelengths.

The utility of our summary SWF lies in the prediction of CDOM photobleaching with knowledge of the incident energy striking a sample (or water parcel). The SWF (*W*[λ], in units of m J^{-1} nm^{-1}) converts $E_d(\lambda)$ into an effect (PB$_{pred}$[λ], the loss of UV absorbance in units of m^{-1}) per nm when multiplied by the absorbed energy per nm. The wavelength-dependent effect (decreasing CDOM absorbance) is assumed to be due to the increasing proportion of carbon bonds that
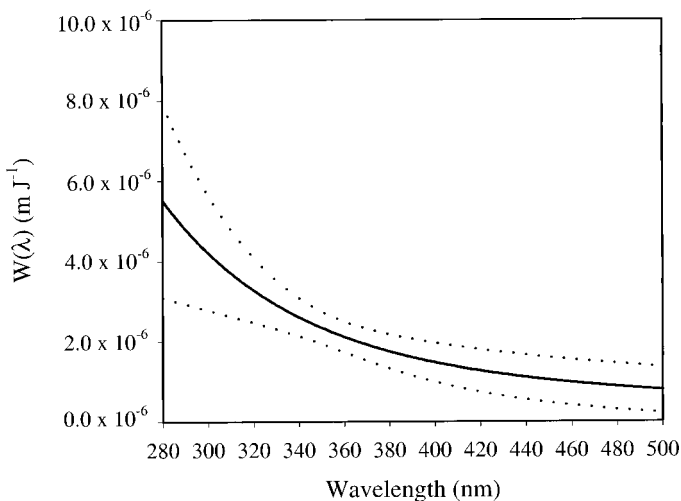

Fig. 6. Wavelength dependence of the summary SWF calculated from individual epilimnial SWFs for photobleaching of CDOM. Dashed lines represent the 95% confidence intervals ($n = 7$).

can be broken by shorter wavelength, high-energy photons. In order to validate the summary SWF, we compared its photobleaching predictions to measured results obtained from similar sunlight exposures of CDOM from other lakes in the region, including Lake Nahuel Huapi, one of the largest and clearest lakes in Patagonia.

We first tested the summary SWF by predicting the results from an exposure experiment of Lake Trebol water to natural sunlight. We used the same method in this experiment as for the cutoff filter experiments used to calculate the SWFs, but these results were not included in the SWF calculations. Figure 7A shows the measured and predicted PB from the 288 nm filter treatment (which approximates full sun conditions) in this separate exposure experiment (Trebol 4). The predicted PB from SWFs generated from the three separate exposures of Trebol CDOM (Trebol 1, 2, and 3) vary by roughly 40%, though the summary SWF (Avg) predicts a value that is not significantly different from the measured PB in the exposure ($p > 0.05$). We used this test as a "first-cut" analysis using an energy spectrum modified (by the cutoff filter) similarly to the spectra used to generate the SWFs.

In our next test, we used the summary SWF to predict PB in experimental exposures of CDOM from several lakes in Argentina, including Trebol and Moreno East. This experiment used quartz tubes without optical filters (i.e., full sun exposure); thus the absorbed energy calculated was close to natural conditions and would test our summary SWF with solar energy incident on the Argentine lakes. This also tested the predictive ability of the summary SWF when applied to CDOM from other lakes. These results are presented in Fig. 7b, which includes CDOM from Lake Escondido, which has more DOC and a higher UV absorbance than either Lake Trebol or Lake Moreno East (Table 2). Lake Nahuel Huapi was included to test the SWF on another clear lake. The summary SWF provided predictions of photobleaching that were not significantly different from the measured photobleaching ($p > 0.05$) for Trebol, Moreno East, and Nahuel
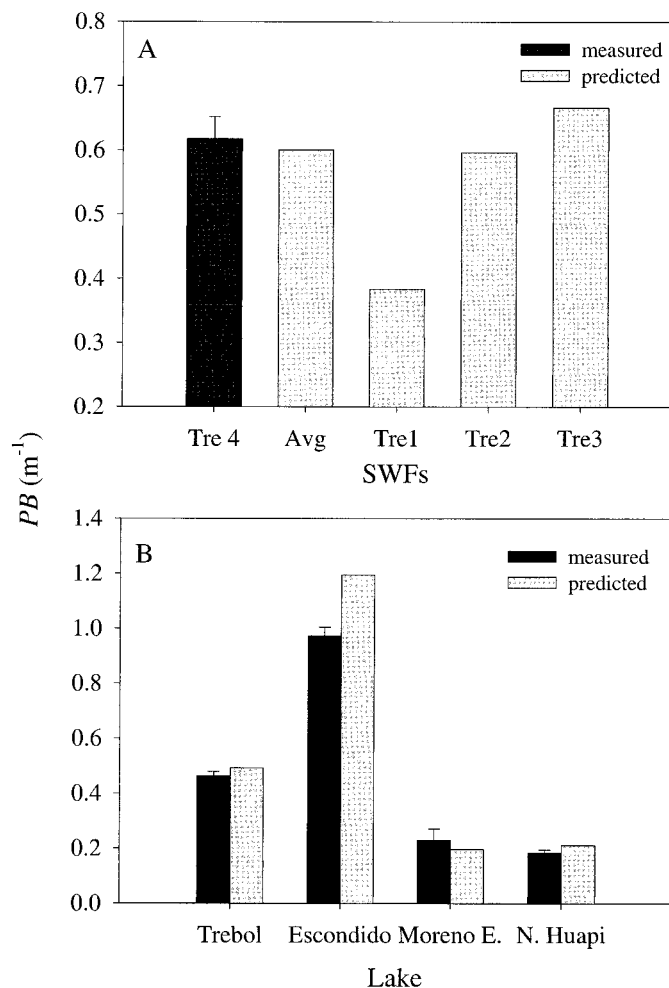
Fig. 7. Comparison of measured and predicted photobleaching (PB) in Patagonian lakes. (A) PB measured in Trebol 4 (Tre 4) exposure (288 nm cutoff filter) compared to PB predicted using individual SWFs from Trebol (Tre 1, 2, 3) and the summary SWF (Avg). (B) Measured and predicted PB (using the summary SWF from Fig. 6) in quartz tube exposures (without cutoff filters) using CDOM from various lakes near Bariloche, Argentina. In both panels, error bars are 95% confidence intervals ($n = 5$).

Huapi. The summary SWF did predict about 20% greater photobleaching than was actually measured for Escondido.

Spectral analysis of SWFs—Analysis of the individual SWF results provided insight into the photoreactivity of CDOM from our various sources with regard to the irradiance spectrum of natural sunlight. Table 4 presents the reaction distribution of PB(λ) over the UV-B, UV-A, and PAR (blue light, 400–500 nm) regions for each CDOM exposure experiment used to calculate the SWFs. These data estimate the region of the solar spectrum most effective at photobleaching CDOM from our various CDOM sources. For all SWFs, the greatest proportion (>50%) of photobleaching was due to the UV-A region of the solar spectrum. This agrees with our estimate of the peak wavelength for photobleaching effect, which was quite similar among all CDOM sources (mean = 330±2 nm; Table 3). Vähätalo et al. (2000;

Table 4. Reaction distribution of PB_{pred} using our multiple SWFs. The percent contributions from each region of the UV and blue light (400–500 nm) are reported. For each SWF used to predict photobleaching, the greatest effect was attributed to the UV-A region, near 335 nm. Averages (AVG) and standard deviations (SD) are shown in the bottom two rows.

	Reaction distribution of photobleaching effect per wavelength region		
SWF*	UVB	UVA	Blue
ME	16%	64%	19%
T1	12%	63%	24%
T2	22%	70%	8%
T3	20%	70%	10%
GE	9%	64%	27%
GH	10%	69%	21%
LE	5%	51%	44%
LM	10%	66%	24%
LH	18%	76%	6%
Bog	5%	53%	42%
Algae	5%	53%	41%
AVG	12%	64%	24%
SD	6%	7%	13%

* Key: ME = Moreno East, T = Trebol (1–3), GE = Giles epilimnion, GH = Giles hypolimnion, LE = Lacawac epilimnion, LM = Lacawac metalimnion, LH = Lacawac hypolimnion.

see their fig. 7E) observed a similar result for photomineralization of lake DOC, whereas Andrews et al. (2000) calculated the maximum oxygen consumption from total water column photooxidation between 335 and 340 nm. Similarly, Graneli et al. (1998) found that UV-A and PAR radiation drove DIC production in Swedish and Brazilian lakes, but found a larger PAR effect than we observed. In contrast to these findings, DeHaan (1993) and Salonen and Vähätalo (1994) observed from broadband experiments that most mineralization of DOC was due to UV-B radiation. Kieber et al. (1990) and Gao and Zepp (1998) have also calculated action spectra suggesting that the high UV-B region (near 320 nm) had the greatest photobleaching effect on DOM. Nevertheless, our results differ by a small margin (10 nm) in a range of the solar spectrum where energy is rapidly decreasing with wavelength.

Prediction of increased photobleaching due to increases in solar UV-B radiation—One central issue in the study of UVR effects on aquatic ecosystems is the degree to which heightened UV-B radiation (due to depletion of stratospheric ozone) might exacerbate the effects. We performed a simple calculation of photobleaching for CDOM exposed to sunlight for 7 d with a 5, 10, and a 25% increase in UV-B irradiance (Table 5). With a 25% increase in UV-B radiation, our calculations predicted an 8% increase in total photobleaching for all lakes except Moreno East (3%). At the 25% level, the relative contribution to photobleaching by UV-B radiation only increased on average by 3%, whereas the relative contribution from UV-A radiation decreased by 1–2%. The relative contribution from PAR remained unchanged. Thus, we conclude that a 25% increase in UV-B radiation from reduced stratospheric ozone concentrations may result

Table 5. Predicted increases in CDOM photobleaching due to increased incident UV-B radiation from depletion of stratospheric ozone for lakes in Patagonia, Argentina.

Predicted increase in UV-B	Predicted increase in photobleaching			
	Trebol	Escondido	E. Moreno	Nahuel Huapi
5%	5.7%	5.7%	0.6%	5.6%
10%	6.4%	6.4%	1.2%	6.1%
25%	8.4%	8.4%	3.0%	7.7%

in roughly a 10% increase of CDOM photobleaching in lake water. We know of no other report that has demonstrated such findings based on SWFs; however, our results agree with radiation amplification factors (RAF) computed for other CDOM photoreactions by Madronich (1995). The RAF represents the fractional change in a photochemical or photobiological process normalized to an assumed fractional change in total ozone.

Comparisons to other photochemical action spectra—The quantum yield spectra (QY) derived from our summary SWF for photobleaching (by conversion of energy to photons) are comparable with other reported QY for various photochemical processes (Fig. 8). Our QY spectrum was similar in slope (−0.0108) to the QY spectrum for photochemical mineralization of DOC from a humic lake reported by Vähätalo et al. (2000; slope = −0.0121 ± 0.00016) but was steeper than the apparent QY for CDOM photobleaching reported by Whitehead et al. (2000). However, the QY for photobleaching reported by Kieber et al. (1990) has a much steeper slope than our QY, suggesting a smaller effect from UV-A radiation. Moreover, Valentine and Zepp (1993) and Moore et al. (1993) reported quantum yields for CO and H_2O_2 production that were highest for UV-B wavelengths, although they note that UV-A and blue light were most responsible for production of these photoproducts. They attribute the greater importance of the UV-A and blue light wavelengths to the greater photon fluence at these wavelengths. The discrepancy between our results and those of Kieber et al. (1990) may be due to the chemical nature of CDOM, which may be quite different in various freshwater ecosystems, and likely varies on a seasonal basis due to prior photobleaching (*see below*).

Photoreactivity of CDOM—Deviation of the summary SWF from the Planck "slope" suggests that seasonal changes in composition and source may modify the photoreactivity of CDOM. We define *photoreactivity* as the change in the average dissolved absorption coefficient divided by the total absorbed energy in an exposed sample (expressed as m J^{-1} × 10^{-6}). We observed wide variation in the photoreactivity of our CDOM sources (Fig. 9). The highest photoreactivity (~5.5 × 10^{-6} m J^{-1}) was observed for the algae and bog samples, whereas the lowest photoreactivity (1.4 × 10^{-6} m J^{-1}) was observed for the Trebol 1 and Moreno East samples. Another pattern that emerges is that all lake CDOM samples exhibited lower photoreactivity than did the CDOM source end members. The average photoreactivity of the lake
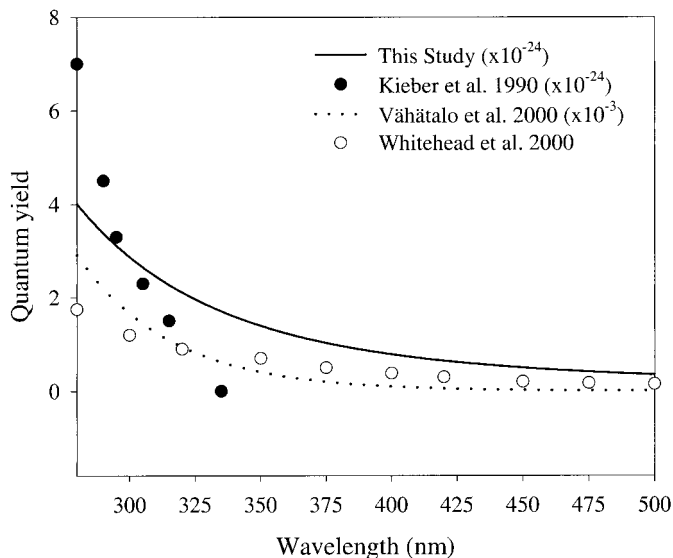

Fig. 8. Comparison of our quantum yield for photobleaching with other published quantum yields for CDOM photobleaching (Kieber et al. 1990; Whitehead et al. 2000) and DOC mineralization (Vähätalo et al. 2000).

CDOM samples was roughly 50% of the algae and bog CDOM samples.

Previous photobleaching history may be the driving force behind much of the difference in CDOM photoreactivity. In Lake Lacawac, for example, the epilimnion CDOM photoreactivity was lower than the metalimnion photoreactivity that was, in turn, lower than the hypolimnion photoreactivity. Thus, photoreactivity appeared to increase with depth in this lake. The Lacawac epilimnion CDOM had been exposed
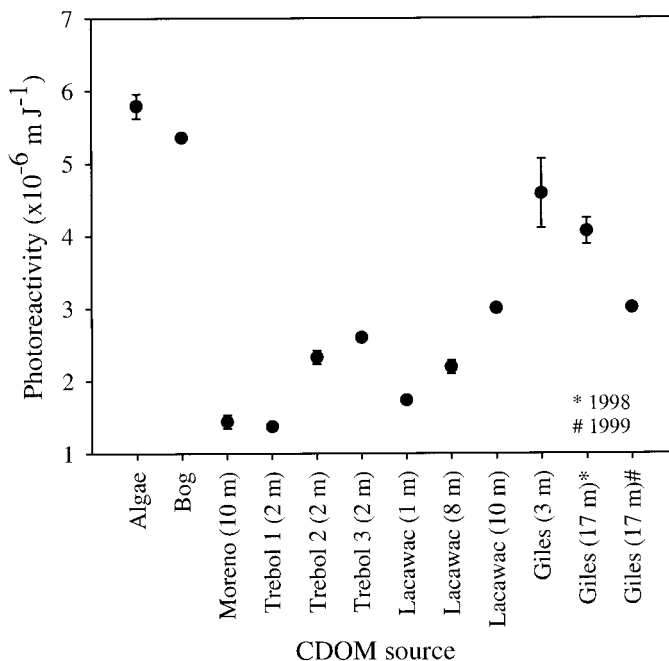

Fig. 9. Photoreactivity of various CDOM sources. Error bars are 95% confidence intervals (*n* = 5). *See text for explanation.*

to photobleaching prior to collection at midsummer. At the time of collection, the average absorption coefficient for the epilimnion (3.16 m^{-1}) was nearly 50% less than that of the metalimnion (5.84 m^{-1}) and roughly 66% less than that of the hypolimnion (10.23 m^{-1}). At spring turnover, prior to substantial photobleaching, the average absorption coefficient was 9.88 m^{-1}; the deviation from this value during summer stratification suggests that sunlight exposure of the surface waters (epilimnion and metalimnion) decreased the photoreactivity. The high photoreactivity of the bog and algae CDOM probably resulted from the absence of previous sunlight exposure, which may serve to explain why the S_w calculated for these SWFs were quite shallow, and in the case of the bog CDOM, not significantly different from zero. We expect a steeper slope in the SWF to reflect a greater spectral dependence for photobleaching per unit absorbed energy toward the UV-B region. Given this, our results suggest that the unexposed, hypolimnion samples were more UV-B photoreactive than the surface samples.

Aside from photobleaching history, the composition of chromophoric matter may also influence the photoreactivity. In the hypolimnion of Lake Lacawac, for example, the major source of chromophoric matter is CDOM from the bog. Laurion et al. (2000) found that epilimnial a_{CDOM}(320) in mountain lakes with low allochthonous input was significantly lower than in lakes with high allochthonous input. However, autochthonous productivity and possibly complexed iron, which occurs in the anoxic hypolimnion, may also contribute chromophoric matter (Osburn et al. 2001). Thus, the higher photoreactivity in the Lacawac hypolimnion CDOM may result from the combination of humic compounds originating in the bog, dissolved iron, or lack of previous sunlight exposure.

For this study, we did not attempt to estimate the mixing between water masses. Strong thermal stratification develops in Lake Giles and Lake Lacawac in early June, and the depths were chosen to clearly delineate between the surface mixed layer and the bottom layer in each lake. Morris and Hargreaves (1997) have noted a seasonal trend in dissolve absorbance in these lakes, reporting that hypolimnion DOC retains the ''spring-like'' absorbance of CDOM measured in the spring during turnover.

The observed increase in photoreactivity of the Lake Trebol epilimnion (with seasonal progression) suggests an input of photoreactive CDOM during the 6-week study period. This conclusion is supported by a 15% increase in water column $a_{CDOM}(\lambda)$ observed in Lake Trebol during the study. We attribute the increase in Trebol CDOM to input from macrophyte senescence and decomposition near our collection site. This CDOM may have high photoreactivity similar to that observed in our bog CDOM sample.

Comparison of the epilimnion and hypolimnion samples in Lakes Giles and Lacawac consistently showed that the UV-B is less important to overall photobleaching in the epilimnion (5% for both lakes) than in the hypolimnion (10 and 18%, respectively; Table 4). In contrast, the importance of blue light was greater in the epilimnion (44% for both lakes) than in the hypolimnion (30 and 21% for Giles, 6% for Lacawac). The shift in the importance of UV-B versus blue light in photobleaching would suggest a steeper slope to the SWF, which is what we observed in these samples (Fig. 4).

Conclusion

To our knowledge, the results we have presented on the spectral dependence of solar UVR photobleaching of CDOM from natural waters have not been demonstrated previously, and they emphasize the importance of our SWF in determining both the spectral dependence of CDOM photobleaching and the photoreactivity of CDOM. This knowledge is crucial because current models of photochemical reactions (from DIC production to photobleaching) use a ''static'' action spectrum usually developed for one particular CDOM sample. Thus, these models may be inaccurate with respect to changes in the spectral sensitivity of the quantum yields for a given process.

Our approach to the calculation of SWFs used the decrease in the dissolved absorption coefficient integrated over the UV-B and UV-A wavebands (280 to 400 nm) and includes contribution from the blue light region, up to 500 nm. Previous investigations into photobleaching of natural waters typically report loss of absorbance at individual wavelengths. For example, Morris and Hargreaves (1997) used $a_{CDOM}(\lambda)$ at 320 and 380 nm to represent photobleaching in the UV-B and UV-A regions, respectively. Other workers have used similar estimations of photobleaching (Strome and Miller 1978; Kieber et al. 1989; Lindell et al. 1995; Vodacek et al. 1997). Since our approach averaged the loss of absorbance over the entire absorbance spectrum of CDOM, we feel this method provides a good summary of the change in the entire absorbance spectrum of CDOM, although our approach does not account for the spectral shifts in the CDOM absorbance spectrum after photobleaching.

Although we were able to predict accurately the responses in the photobleaching of CDOM from multiple lakes, the utility of SWFs to predict photobleaching in the natural environment carries many assumptions. One is that the photoreactivity of CDOM does not change upon exposure to sunlight. This is unlikely as chromophores are degraded upon exposure. Thus, seasonal variations in CDOM photoreactivity not accounted for by our model may result in an overestimation of photobleaching in natural waters, as we observed for Lake Escondido. Furthermore, our models are based on static experiments with no input of fresh CDOM and no influence of biological processes such as microbial metabolism. Several studies have shown that bacteria may enhance the degradation of dissolved organic material exposed to UV radiation (Amador et al. 1991; Lindell et al. 1995; Moran et al. 2000), and it is possible that this may further reduce its photoreactivity. Given these assumptions, we suggest that prior sunlight exposure is a good basis for determining a summary SWF, but that the SWF should only be applied to predictions of photobleaching in surface waters of lakes, where CDOM is being exposed to sunlight. The photobleaching history of the CDOM is likely to be most important in determining its photoreactivity, contributions of CDOM from allochthonous and autochthonous sources notwithstanding. Our analysis of photobleaching also suggested

that allochthonous and autochthonous CDOM sources have similar photoreactivity, something not observed by Thomas and Lara (1995) for CDOM produced by marine algae. In conclusion, we have demonstrated that a SWF can be determined easily for a natural water body, and that a summary SWF may be used to estimate changes in surface water CDOM dissolved absorbance due to photobleaching by solar UVR.

References

AMADOR, J. A., M. ALEXANDER, AND R. G. ZIKA.. 1991. Degradation of aromatic-compounds bound to humic-acid by the combined action of sunlight and microorganisms. Environ. Toxicol. Chem. **10:** 475–482

ALLARD, B., H. BORÉN, C. PETTERSON, AND G. ZHANG. 1994. Degradation of humic substances by UV irradiation. Enivron. Int. **20:** 97–101.

ANDREWS, S. A., S. CARON, AND O. C. ZAFIRIOU. 2000. Photochemical oxygen consumption in marine waters: A major sink for colored dissolved organic matter? Limnol. Oceanogr. **45:** 267–277.

BOUCHER, N., AND B. B. PREZELIN. 1996. An in situ biological weighting function for UV inhibition of phytoplankton carbon fixation in the Southern Ocean. Mar. Ecol. Prog. Ser. **144:** 223–236.

BRICAUD, A., A. MOREL, AND L. PRIEUR. 1981. Absorption by dissolved organic matter of the sea (yellow substance) in the UV and visible domains. Limnol. Oceanogr. **16:** 43–53.

CULLEN, J. J., AND P. J. NEALE. 1997. Biological weighting functions for describing the effects of ultraviolet radiation on aquatic systems. *In* D. P. Hader [ed.], The effects of ozone depletion on aquatic ecosystems. Academic.

———, ———, AND M. P. LESSER. 1992. Biological weighting function for the inhibition of phytoplankton photosynthesis by ultraviolet radiation. Science **258:** 646–650.

DEHAAN, H. 1993. Solar UV-light penetration and photodegradation of humic substances in peaty lake water. Limnol. Oceanogr. **38:** 1072–1076.

GAO, W., AND R. G. ZEPP. 1998. Factors influencing photoreactions of dissolved organic matter in a coastal river of the Southeastern United States. Enivron. Sci. Technol. **32:** 2940–2946.

GRANELI, W., M. LINDELL, M. BIAS, AND F. ESTEVES. 1998. Photoproduction of dissolved inorganic carbon in temperate and tropical lakes—dependence on wavelength band and dissolved organic carbon concentration. Biogeochemica **43:** 175–195.

HADER, D.-P., H. D. KUMAR, R. C. SMITH, AND R. C. WORREST. 1998. Effects on aquatic ecosystems. J. Photochem. Photobiol. B **46:** 53–68.

———, AND R. C. WORREST. 1991. Photobiology school: Effects of enhanced solar ultraviolet radiation on aquatic ecosystems. Photochem. Photobiol. **53:** 717–725.

HONGVE, D., AND ÅKESSON, G. 1996. Spectrophotometric determination of water colour in Hazen units. Water Res. **30:** 2771–2775.

KARENTZ, D., AND OTHERS. 1994. Impact of UV-B radiation on pelagic freshwater ecosystems: Report of the working group on bacteria and phytoplankton. Arch. Hydrobiol. Ergeb. Limnol. **43:** 1–226.

KIEBER, D. J., J. MCDANIEL, AND K. MOPPER. 1989. Photochemical source of biological substrates in seawater: Implications for carbon cycling. Nature **341:** 637–639.

KIEBER, R. J., X. ZHOU, AND K. MOPPER. 1990. Formation of carbonyl compounds from UV-induced photodegradation of humic substances in natural waters: Fate of riverine carbon in the sea. Limnol. Oceanogr. **35:** 1503–1515.

KIRK, J. T. O. 1994. Light and photosynthesis in aquatic ecosystems, 2nd ed. Cambridge.

———, AND OTHERS. 1994. Measurements of UV-B radiation in two freshwater lakes: An instrument comparison. Ergeb. Limnol. **43:** 71–99.

KOUASSI, A. M., AND R. G. ZIKA. 1992. Light-induced destruction of the absorbance property of dissolved organic matter in seawater. Toxicol. Environ. Chem. **35:** 195–211.

LAURION, I., M. VENTURA, J. CATALAN, R. PSENNER, AND R. SOMMARUGA. 2000. Attenuation of ultraviolet radiation in mountain lakes: Factors controlling the among- and within-lake variability. Limnol. Oceanogr. **45:** 1274–1288.

LINDELL, M., W. GRANELI, AND L. TRANVIK. 1995. Enhanced bacterial growth in response to photochemical transformation of dissolved organic matter. Limnol. Oceanogr. **40:** 195–199.

———, AND H. RAI. 1994. Photochemical oxygen consumption in humic waters. Ergeb. Limnol. **43:** 145–155.

MADRONICH, S., R. L. MCKENZIE, M. CALDWELL, AND L. O. BJORN. 1995. Changes in ultraviolet radiation reaching the Earth's surface. Ambio **24:** 143–152.

MILLER, W. M. 1998. Effects of UV radiation on aquatic humus: Photochemical principles and experimental considerations, p. 125–141. *In* D. O. Hessen and L. Tranvik [eds], Aquatic humic substances: Ecology and biogeochemistry. Ecological Studies 133. Springer-Verlag.

———, AND R. G. ZEPP. 1995. Photochemical production of dissolved inorganic carbon from terrestrial organic matter: Significance to the oceanic organic carbon cycle. Geophys. Res. Lett. **22:** 417–420.

MOLOT, L., AND P. J. DILLON. 1997. Colour-mass balances and colour-dissolved organic carbon relationships in lakes and streams in central Ontario. Can. J. Fish. Aquat. Sci. **54:** 2789–2795.

MOORE, C. A., C. T. FARMER, AND R. G. ZIKA. 1993. Influence of the Orinoco River on hydrogen peroxide distribution and production in the eastern Caribbean. J. Geophys. Res. **98:** 2289–2298.

MORAN, M. A., W. M. SHELDON, JR., AND R. G. ZEPP. 2000. Carbon loss and optical property changes during long-term photochemical and biological degradation of estuarine dissolved organic matter. Limnol. Oceanogr. **45:** 1254–1264.

———, AND R. G. ZEPP. 1997. Role of photoreactions in the formation of biologically labile compounds from dissolved organic matter. Limnol. Oceanogr. **42:** 1307–1316.

MORRIS, D. P., AND B. R. HARGREAVES. 1997. The role of photochemical degradation of dissolved organic carbon in regulating the UV transparency of three lakes on the Pocono Plateau. Limnol. Oceanogr. **42(2):** 239–349.

———, AND OTHERS. 1995. The attenuation of solar UV radiation in lakes and the role of dissolved organic carbon. Limnol. Oceanogr. **40:** 1381–1391.

OSBURN, C. L., D. P. MORRIS, K. A. THORN, AND R. E. MOELLER. In press. Chemical and optical changes in freshwater dissolved organic matter exposed to solar radiation. Biogeochem.

RECHE, I., M. L. PACE, AND J. J. COLE. 1999. Relationship of trophic and chemical conditions to photobleaching of dissolved organic matter in lake ecosystems. Biogeochem. **44:** 259–280.

RUNDEL, R. D. 1983. Action spectra and estimation of biologically effective UV radiation. Physiol. Plant. **58:** 360–366.

SALONEN, K., AND A. VÄHÄTALO. 1994. Photochemical mineralization of dissolved organic matter in Lake Skjervatjern. Environ. Int. **20:** 307–312.

SETLOW, R. B. 1974. The wavelengths in sunlight effective in producing skin cancer: A theoretical analysis. Proc. Natl. Acad. Sci. USA **71:** 3363–3366.

STROME, D. J., AND M. C. MILLER. 1978. Photolytic changes in dissolved humic substances. Verh. Int. Verein. Limnol. **20:** 1248–1254.

THOMAS, D. N., AND R. J. LARA. 1995. Photodegradation of algal derived dissolved organic carbon. Mar. Ecol. Prog. Ser. **116:** 309–310.

VÄHÄTALO, A. V., M. SALKINOJA-SALONEN, P. TAALAS, AND K. SALONEN. 2000. Spectrum of the quantum yield for photochemical mineralization of dissolved organic carbon in a humic lake. Limnol. Oceanogr. **45:** 664–676.

VALENTINE, R. L., AND R. G. ZEPP. 1993. Formation of carbon monoxide from the photodegradation of terrestrial dissolved organic carbon in natural waters. Environ. Sci. Technol. **27:** 409–412.

VODACEK, A., N. V. BLOUGH, M. D. DEGRANDPRE, E. T. PELTZER, AND R. K. NELSON. 1997. Seasonal variation of CDOM and DOC in the Middle Atlantic Bight: Terrestrial inputs and photooxidation. Limnol. Oceanogr. **42:** 674–686.

WHITEHEAD, R. F., S. DE MORA, S. DEMERS, M. GOSSELIN, P. MONFORT, AND B. MOSTAJIR. 2000. Interactions of ultraviolet-B radiation, mixing, and biological activity on photobleaching of natural chromophoric dissolved organic matter: A mesocosm study. Limnol. Oceanogr. **45:** 278–291.

WILLIAMSON, C. E., AND H. E. ZAGARESE. 1994. The impact of UV-B radiation on pelagic freshwater ecosystems. Arch. Hyrobiol. Suppl. **43:** IX–XI.

ZEPP, R. G. 1988. Environmental photoprocesses involving natural organic matter, p. 193–214. *In* F. H. Frimmel and R. F. Christman [eds.], Humic substances and their role in the environment. Wiley.